Application of self-assembled hemispherical microlasers as gas sensors

V. D. Ta,[1] R. Chen,[1] D. M. Nguyen,[1] and H. D. Sun[1,2,a)]
[1]*Division of Physics and Applied Physics, School of Physical and Mathematical Sciences, Nanyang Technological University, Singapore 637371, Singapore*
[2]*Centre for Disruptive Photonic Technologies (CDPT), Nanyang Technological University, Singapore 637371, Singapore*

(Received 17 October 2012; accepted 7 January 2013; published online 23 January 2013)

Dye-doped hemispherical resonators are self-assembled on a distributed Bragg reflector based on hydrophobic effect. The size of hemispheres can be well-controlled with diameters ranging from 5 to 150 μm. Upon optical pumping, whispering gallery mode laser emission with transverse magnetic polarization is observed from the hemispheres. Application of the microlasers as refractive index gas sensors has been demonstrated by detecting the spectrum shift of the lasing mode, and the sensitivity higher than 130 nm/RIU is achieved. Our approach provides an effective technique to obtain high quality microlasers and opens an opportunity to employ the cost effective microlasers as high sensitive sensors. © *2013 American Institute of Physics*. [http://dx.doi.org/10.1063/1.4788751]

Low loss optical resonators are always the pursuit for researchers in optics and photonics.[1] Among different configurations, whispering gallery cavities (WGC) have attracted increasing research attentions due to their high quality (Q) factor, small mode volume,[1,2] and a key factor for both fundamental studies, such as strong coupling between light and matter[3] as well as applications including laser sources,[4–11] optical filters,[12] and high sensitive sensors.[13–17]

It is well-known that light can be well-trapped inside a WGC by multiple total internal reflections.[7] Structures with smooth surface and high symmetric order are typically desirable to realize WGC.[6–9] Interestingly, these structures can be readily obtained by self-assembled process, such as water, organic, and liquid crystal droplets, which have been demonstrated for high Q factor WGC. In particular, polymer hemispherical microresonators on top of a distributed Bragg reflector (DBR) have been fabricated,[18] and the proof-of-concept demonstration of three-dimensional-confined whispering gallery mode (WGM) lasing have been achieved.[10,11] Further detailed investigations of these structures, such as fabrication approaches, lasing characteristics, and their possible applications are needed to appreciate their potential as photonic devices.

In this Letter, we report an effective technique for mass production of polymer hemispherical resonators on DBR substrates,[10] which are practically used for high Q microlasers and ultra-sensitive refractive index gas sensors. Self-assembled, high uniformity, and well-aligned resonators with tunable sizes ranging from 5 to 150 μm can be easily obtained. Under optical pumping, low threshold laser emission with transverse magnetic (TM) polarization is observed from dye-doped hemispheres at room temperature. The lasing mechanism is well-explained by WGM theory. Moreover, the hemisphere lasers can be served as good refractive index gas sensors with sensitivity higher than 130 nm per refractive index unit (RIU).

Hemispherical structures are obtained by combining highly uniform polymer microfibers with strong hydrophobic effect. The fibers are directly drawn from a solution synthesized as follows. First, poly(methyl methacrylate) (PMMA) is dissolved in dichloromethane with concentration of about 10 wt. %. Then, the epoxy resin[10] and Rhodamine B (RhB) are added. Weight ratio of epoxy and PMMA is approximately 6:1 and concentration of RhB is around 0.2 wt. %. A layer of mixed 1H, 1H, 2H, 2H-perfluorooctyltriethoxysilane[18] and dichloromethane with ratio 1:4 in volume is coated to increase the hydrophobic effect of the DBR surface. A drop of the mixture is deposited on the DBR surface and uniformly spreads with a soft felt[18] to form the layer (the so-called hydrophobic layer). To obtain hemispherical structures, a RhB-doped polymer fiber is fabricated by a direct drawing technique[5] and subsequently placed on the hydrophobic DBR's surface. Figure 1(a) illuminates an optical image of a fiber on the DBR just 2 min after the fiber is placed on. Due to the hydrophobic layer and surface tension of the fiber's material, various parts along the fiber are shrunk [Fig. 1(b)] and then simultaneously breaks into numerous small pieces with similar lengths [Fig. 1(c)]. Several minutes later, these pieces are self-assembled to form hemispherical structures with circular shapes [Fig. 1(d)]. Size of hemispheres is a function of the fiber's diameter, which can be well-controlled by the drawing speed.[5] As shown in Figures 1(e)–1(g), hemispheres with different diameters (D) are readily obtained. The hemispheres are well-aligned and with high uniformity.

The self-assembled process is time-dependent. The total time (T_{total}) for the hemisphere formation counted from the fiber placed on the DBR depends on two factors: (i) weight ratio of the epoxy and PMMA (WR_{ep}) and (ii) size of the fiber. It is found that if WR_{ep} is below 4:1, the self-assembled process cannot be achieved. When increasing WR_{ep} from 4:1 to 8:1, the self-assembling process takes place with a decreasing of T_{total}. For fibers with similar diameters of about 50 μm, T_{total} might take around 10 h for $WR_{ep} \sim 4:1$ but only 10 min for $WR_{ep} \sim 8:1$. In the case that WR_{ep} is larger than 8:1, the fiber is extremely difficult to draw as concentration of PMMA

a)Author to whom correspondence should be addressed. Email: hdsun@ntu.edu.sg.

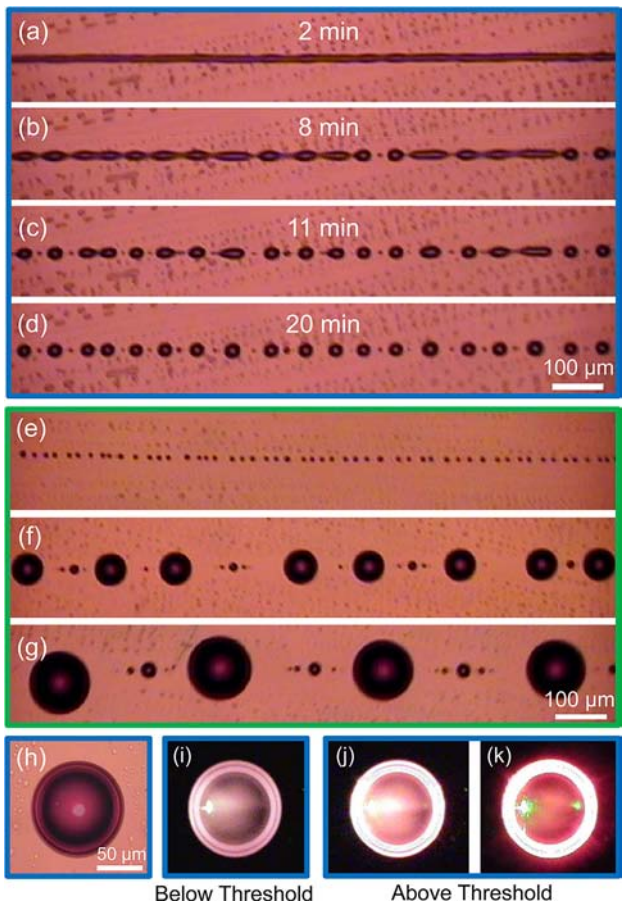

FIG. 1. (a)–(d) Time-dependence of the self-assembled process. The time is counted when the fiber is placed on the DBR substrate. (e)–(g) Demonstration of well-aligned hemispheres with increasing sizes from around 10 to 100 μm. (h) Optical image of a typical hemisphere and (i)–(k) its photoluminescence images with increasing excitation. Intensive emission at the outer part of the hemisphere in (j) and (k) predicts the WGM lasing mechanism.

in the composition is too low. For fibers with different sizes, it is found that the process finishes quickly for a small fiber and takes more time for a bigger one. For instance, with fixed $WR_{ep} \sim 6{:}1$, T_{total} takes around 20, 70, and, 110 min for the fibers with diameter about 20, 60, and 100 μm, respectively. In this work, all presented hemispheres were based on the solution with $WR_{ep} \sim 6{:}1$. To make these hemispheres ready for subsequent optical measurements, it was baked in an oven at 60 °C for about 90 min and additional dried in the air at room temperature for 2–3 days, which helps to evaporate the solvent and stabilize the hemispheres' structure.

A green pulse laser (wavelength: 532 nm, pulse duration: 1 ns, and repetition rate: 60 Hz) was used to excite the hemispheres. Excitation spot is around 1.2 mm in diameter. Figures 1(h)–1(k) shows images of a typical hemisphere under optical excitation with increasing pump pulse energy (PPE). The hemisphere above lasing threshold [Figs. 1(j) and 1(k)] exhibits much higher brightness compared with the one below threshold [Fig. 1(i)]. Moreover, the observation of an extremely intense light with ring shape located at the outer part of the hemisphere in Figs. 1(j) and 1(k) predicts the cavity may due to WGMs. It is important to note that the DBR substrate plays a critical role to achieve lasing emission. It consists of 27 pairs of quarter-wave-thick SiO_2 and TiO_2 layers. The stop-band width of the DBR is about 140 nm with a reflectivity up to about 99.5% at 630 nm.[10] Due to the high-reflectivity, the DBR significantly prevents the optical field of WGMs from leaking to the glass substrate.[11]

Emission from the excited hemispheres can be collected by suitable objectives, and the optical signal is delivered into a 750 mm monochromator connected with a charged coupled device (CCD) for spectrum recording. Figure 2(a) illuminates a schematic optical setup for indentifying polarization property of laser emission by a polarizer. The polarization and laser pulse energy were fixed during the experiment. The emission is collected from the edge of the hemisphere with a spectral resolution of about 50 pm. We recorded lasing intensity after the polarizer. Figure 2(b) presents a spectrum from a hemisphere with $D \sim 130\,\mu$m as a function of rotation angle (α). It can be seen that the lasing reaches maximum intensity when $\alpha = 0°$ and 180° while totally disappears when $\alpha = 90°$. The integrated lasing intensity as a function of α is presented in the inset, which indicates that the experimental data can be well-fitted by Malus' law. It is, therefore, concluded that there exists only TM polarization of the laser emission. Visually, for the TM polarization, the electric field oscillates in a radial direction as schematically illuminated in Fig. 2(a).[7] Various hemispheres were studied and identical TM polarization characteristics were observed. In addition, under extremely high excitation energy, different lasing modes with transverse electric (TE) polarization can also be detected. However, the lasing emission with TE polarization is several orders of magnitude weaker than TM polarization, which might ascribe to much higher diffraction lost of the TE light.[19]

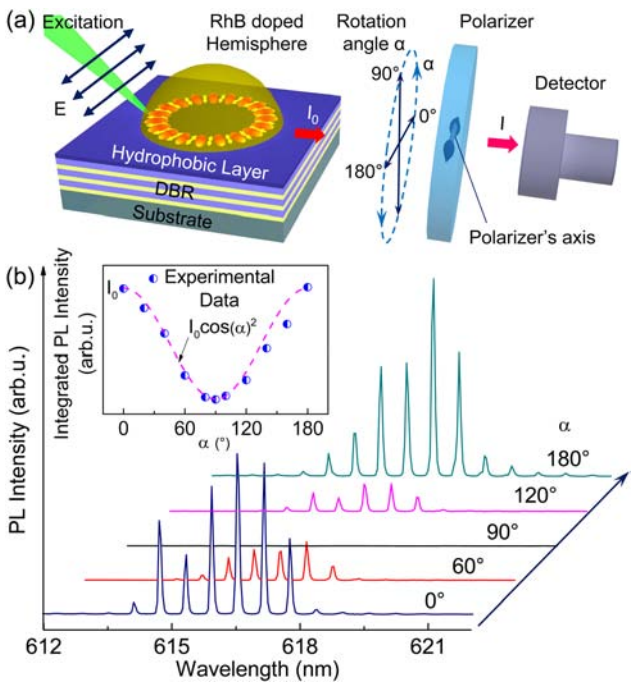

FIG. 2. (a) Schematic diagram of the optical measurement setup. Electric field oscillation (E) of the excitation laser is fixed during the experiment. It is parallel to the axis of polarizer at an initial measurement ($\alpha = 0°$). The arrows inside the hemisphere indicate electric field oscillation of WGMs (red patterns). (b) The lasing spectra as a function of rotation angle of polarizer α. The inset presents a dependence of integrated lasing intensity with α.

Low threshold is an important parameter of microlasers for photonic integrated circuits.[20] For our structures, the lasing threshold is generally below 45 $\mu J \cdot cm^{-2}$. For instance, as shown in Fig. 3(a), the lasing threshold of a studied hemisphere with $D \sim 104\,\mu m$ is around 380 nJ (relates to fluence per pulse of $\sim 34\,\mu J \cdot cm^{-2}$). The inset shows a photoluminescence (PL) spectrum just above threshold, which contains a weak spontaneous emission (broad linewidth) together with lasing emission (two sharp peaks). Lasing modes can be explained by using an asymptotic solution for TM polarization with mode order $r = 1$.[9,21] Considering $D = 104.01\,\mu m$ (close to a value estimated from optical image), refractive index of surrounding medium $n_{air} = 1$, and effective refractive index of the hemisphere $n_{eff} = 1.46$ then lasing modes are well-fitted with mode numbers $m = 759$–762 as indexed in Fig. 3(b).

Size-dependent characteristics are briefly discussed in Fig. 3(c) where spectra of three hemispheres with different sizes are presented. It can be seen that when D decreases, the number of lasing modes decreases together with the increase of free spectral range (FSR). In principle, when the FSR is comparable with the width of lasing region, single mode lasing can be obtained.[6] For our hemispheres, single mode lasing is usually observed when $D \sim 10\,\mu m$, which is similar with previous report on microdrop laser.[6] The achievement of single longitudinal mode laser might find potential application in laser metrology.[11]

WGM technology, which is label-free and ultrasensitive, has been widely used for biological and chemical sensing.[14] Principle of the sensing is based on the interaction between evanescent waves of the WGMs and molecules attached on the cavity's surface, and characterized by a shift of resonant mode.[13–17] Following this idea, we demonstrate an application of the hemisphere laser as refractive index gas sensor.

A hemisphere with $D \sim 53\,\mu m$ was fixed at the bottom of a glass beaker, which was firmly sealed by a parafilm. A small window was opened to allow the excitation, collection of emission, and the loading of sensing vapor. In addition, a lower frequency (20 Hz) of pulse laser was chosen for excitation to have better emission stability from the hemisphere.

Acetone vapor is served as a loading gas to change the surrounding environment of the hemisphere. The beaker was pumped with this vapor through the window for about 15 s. After that, the vapor source was removed. Subsequently, the hemisphere was constantly excited for 4 s, and the spectrum is continuously recording by the CCD with integrated time of 100 ms. Figure 4(a) shows spectra from the hemisphere within 4 s excitation together with a high resolution part of the spectrum in Fig. 4(b). It can be seen that the resonant modes exhibit a gradual blue-shift with time [the so-called diffusion time of acetone vapor (T_d)]. This observation can be well-explained by the decreasing of refractive index of the surrounding medium as function of time. As can be imaged, the acetone vapor is diffusing from the beaker through the open window to the air outside, which leads to the decrease of the acetone vapor concentration and then the refractive index of the medium. The process continues till the surrounding environment of the hemisphere is pure air. Therefore, it is important to compare the spectrum before the vapor adding and after the vapor is totally diffused. We have made the

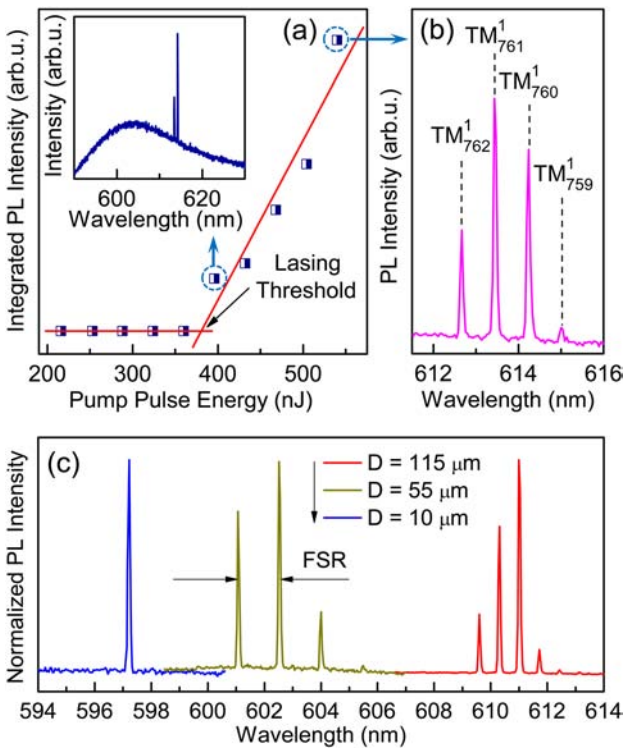

FIG. 3. (a) Evaluation of lasing threshold from hemisphere with $D \sim 104\,\mu m$. The inset demonstrates a spectrum just above lasing threshold. (b) Lasing mode determination based on WGM theory. (c) Lasing spectra of hemispheres with different diameters.

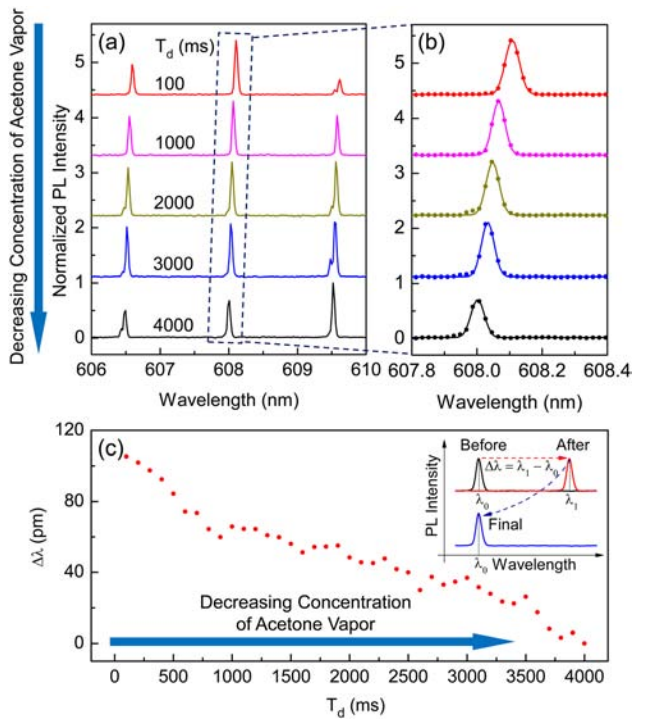

FIG. 4. (a) Lasing spectra from the hemisphere versus diffusion times of acetone vapor (T_d) and (b) close-up image of the spectra near 608 nm. The linewidth of lasing mode is around 0.06 nm, corresponding to $Q \sim 1 \times 10^4$. (c) Dynamic shift of lasing mode monitoring near 608 nm with T_d. The inset schematically illuminates resonant mode and its position at the time: "Before"—before the sensing vapor is added (black), "After"—after the vapor is added (red), and "Final"—the vapor is completed diffused (blue).

comparison and found that the resonant modes are exactly the same as schematically drawn in the inset of Fig. 4(c). We, therefore, conclude from the reversible process that the blue-shift of resonant modes is related to the decrease of refractive index (or concentration of acetone vapor) inside the beaker.

Dynamic change of the resonant modes is plotted in Fig. 4(c). It can be seen that the shifted value ($\Delta\lambda$) linearly decreases with T_d. The fluctuation of the spectral position might due to the non-uniform diffusion of acetone vapor. The maximum shift can be determined as 109 pm corresponding to a variation of refractive index of about 8×10^{-4} RIU. Therefore, the sensitivity of the gas sensor should be better than 130 nm/RIU, which is one order of magnitude higher than the reported data in Ref. 15. The performance of this sensor is ascribed to the Q factor of the hemisphere. In our previous work (Ref. 10), we have demonstrated that the Q factor of hemispheres increase linearly with their size. Therefore, a bigger hemisphere is expected to have a better sensitivity. Prior to practical application, the quantitative relationship between the gas sensitivity and the spectral shift should be established. Nevertheless, this achievement opens an opportunity to employ the cost effective microlasers as high sensitive optical sensors.

In conclusion, we have demonstrated the fabrication and optical property investigation of the self-assembled hemispherical microlasers with different sizes under pulse laser excitation. Single and multiple mode lasing are obtained with linewidth as narrow as 0.06 nm. Application of the microlasers as refractive index gas sensor has been performed by detecting the shifting of lasing mode, and the sensor's sensitive higher than 130 nm/RIU is achieved. Owing to the simple fabrication, excellent laser performances, and high sensitive, our findings provide a promising candidate for fundamental investigation of light-matter interaction and point out their potential applications as photonic devices.

Support from the Singapore Ministry of Education through the Academic Research Fund (Tier 1) under Project No. RG63/10 and from the Singapore National Research Foundation through the Competitive Research Programme (CRP) under Project No. NRF-CRP6-2010-02 is gratefully acknowledged.

[1]K. J. Vahala, Nature **424**, 839 (2003).
[2]A. B. Matsko and V. S. Ilchenko, IEEE J. Sel. Top. Quantum Electron. **12**, 3 (2006).
[3]L. Sun, Z. Chen, Q. Ren, K. Yu, L. Bai, W. Zhou, H. Xiong, Z. Zhu, and X. Shen, Phys. Rev. Lett. **100**, 156403 (2008).
[4]R. Chen, B. Ling, X. W. Sun, and H. D. Sun, Adv. Mater. **23**, 2199 (2011).
[5]V. D. Ta, R. Chen, L. Ma, Y. J. Ying, and H. D. Sun, Laser Photon. Rev. **7**, 133 (2013)
[6]J. Schäfer, J. P. Mondia, R. Sharma, Z. H. Lu, A. S. Susha, A. L. Rogach, and L. J. Wang, Nano Lett. **8**, 1709 (2008).
[7]M. Humar, M. Ravnik, S. Pajk, and I. Muševič, Nature Photon. **3**, 595 (2009).
[8]T.-J. Yim, T. Zentgraf, B. Min, and X. Zhang, J. Am. Chem. Soc. **132**, 2154 (2010).
[9]S. K. Y. Tang, R. Derda, Q. Quan, M. Loncar, and G. M. Whitesides, Opt. Express **19**, 2204 (2011).
[10]V. D. Ta, R. Chen, and H. D. Sun, Adv. Mater. **24**, OP60 (2012).
[11]R. Chen, V. D. Ta, and H. D. Sun, Sci. Rep. **2**, 244 (2012).
[12]A. A. Savchenkov, V. S. Ilchenko, A. B. Matsko, and L. Maleki, IEEE Photon. Technol. Lett. **17**, 136 (2005).
[13]A. M. Armani, R. P. Kulkarni, S. E. Fraser, R. C. Flagan, and K. J. Vahala, Science **317**, 783 (2007).
[14]F. Vollmer and S. Arnold, Nat. Methods **5**, 591 (2008).
[15]I. M. White, H. Oveys, and X. Fan, Opt. Lett. **31**, 1319 (2006).
[16]S. Soria, S. Berneschi, M. Brenci, F. Cosi, G. Nunzi Conti, S. Pelli, and G. C. Righini, Sensors **11**, 785 (2011).
[17]L. He, S. K. Ozdemir, J. Zhu, W. Kim, and L. Yang, Nat. Nanotechnol. **6**, 428 (2011).
[18]J. Haase, S. Shinohara, P. Mundra, G. Risse, V. G. Lyssenko, H. Fröb, M. Hentschel, A. Eychmüller, and K. Leo, Appl. Phys. Lett. **97**, 211101 (2010).
[19]M. Hosoda and T. Shigaki, Appl. Phys. Lett. **90**, 181107 (2007).
[20]M. Humar and I. Muševič, Opt. Express **18**, 26995 (2010).
[21]C. C. Lam, P. T. Leung, and K. Young, J. Opt. Soc. Am. B **9**, 1585 (1992).